University of Kent

Kent Academic Repository

Xiao, Dongrui, Shao, Liyang, Wang, Chao, Lin, Weihao, Yu, Feihong, Wang, Guoqing, Ye, Tao, Wang, Weizhi and Vai, Mang I (2021) *Optical sensor network interrogation system based on nonuniform microwave photonic filters.* Optics Express, 29 (2). p. 2564. ISSN 1094-4087.

Downloaded from

https://kar.kent.ac.uk/92169/ The University of Kent's Academic Repository KAR

The version of record is available from

https://doi.org/doi:10.1364/OE.413990

This document version

Publisher pdf

DOI for this version

Licence for this version

CC BY (Attribution)

Additional information

Versions of research works

Versions of Record

If this version is the version of record, it is the same as the published version available on the publisher's web site. Cite as the published version.

Author Accepted Manuscripts

If this document is identified as the Author Accepted Manuscript it is the version after peer review but before type setting, copy editing or publisher branding. Cite as Surname, Initial. (Year) 'Title of article'. To be published in ***Title of Journal*** , Volume and issue numbers [peer-reviewed accepted version]. Available at: DOI or URL (Accessed: date).

Enquiries

If you have questions about this document contact ResearchSupport@kent.ac.uk. Please include the URL of the record in KAR. If you believe that your, or a third party's rights have been compromised through this document please see our Take Down policy (available from https://www.kent.ac.uk/guides/kar-the-kent-academic-repository#policies).

Research Article | Vol. 29, No. 2 / 18 January 2021 / Optics Express 2564
Optics EXPRESS

Optical sensor network interrogation system based on nonuniform microwave photonic filters

DONGRUI XIAO,[1] LIYANG SHAO,[1,2,5] CHAO WANG,[3,6] WEIHAO LIN,[1,4] FEIHONG YU,[1] GUOQING WANG,[1] TAO YE,[1] WEIZHI WANG,[2] AND MANG I VAI[4]

[1]*Department of Electrical and Electronic Engineering, Southern University of Science and Technology, Shenzhen 518055, China*
[2]*Peng Cheng Laboratory, Shenzhen 518055, Guangdong, China*
[3]*School of Engineering and Digital Arts, University of Kent, Canterbury, UK*
[4]*Department of Electrical and Computer Engineering, Faculty of Science and Technology, University of Macau, Macau 999078, China*
[5]*shaoly@sustech.edu.cn*
[6]*c.wang@kent.ac.uk*

Abstract: Based on the nonuniformly spaced microwave photonic delay-line filter technology, a new design of a generic optical fiber sensor network interrogation platform is proposed and demonstrated. Sensing information from different types of optical sensors embedded in filter taps is converted into the variations of delay time and amplitude of each filter tap individually. Information to be measured can be decoded from the complex temporal impulse response of the microwave photonic filter. As proof-of-concept, our proposed approach is verified by simulations and experimental demonstrations successfully. Four optical sensors of different types are simultaneously interrogated via inverse Fourier transform of the filter frequency response. The experiment results show good linearity between the variation of temporal impulse response and the variations of the twist, the lateral pressure, the transversal loading and the temperature. The sensitivity of the sensors in the proposed platform is -2.130×10^{-5} a.u/degree, 6.1039 ps/kPa, -1.9146×10^{-5} a.u/gram, and 5.1497 ps/°C, respectively. Compared to the conventional optical sensors interrogation system, the presented approach provides a centralized solution that works for different types of optical sensors and can be easily expanded to cover larger optical sensor networks.

Published by The Optical Society under the terms of the Creative Commons Attribution 4.0 License. Further distribution of this work must maintain attribution to the author(s) and the published article's title, journal citation, and DOI.

1. Introduction

Optic fiber sensors received wide range of research interests over the last several decades thanks to their unique characteristics, such as light weight, compactness, immunity to electromagnetic interference, and resistance to chemical corrosion [1]. Most of the interrogation technologies for optical fiber sensors are based on variation of wavelength or power, so the resolution and interrogation speed are limited by the inherent characteristics of optical measuring equipment, such as optical spectrum analyzers (OSA) which suffered from low resolution bandwidths (~gigahertz or hundreds of megahertz) [2]. Meanwhile, microwave photonic techniques have attracted great interest in recent years for their promising contributions in improving the performance of optical sensing systems [2–6]. As the sensing information carried by optical signals is converted to the microwave domain where even low frequency like ~Hz level signal can be easily distinguished by electrical spectrum analyzer (ESA), the interrogation speed and resolution can be significantly enhanced thanks to mature microwave measuring method. On the other hand, the wavelength of

#413990 https://doi.org/10.1364/OE.413990
Journal © 2021 Received 6 Nov 2020; revised 24 Dec 2020; accepted 29 Dec 2020; published 14 Jan 2021

Optics EXPRESS

microwave signal is much larger than that of optical signal, which makes the sensing signal have stronger ability to resist external disturbance.

Microwave-photonics-based optical sensor interrogation technologies can be generally classified into three types.

The first type of microwave-photonics-based optical sensor interrogation technique is based on the photonic time stretch (PTS) concept. For example, by converting the change of optical wavelength to temporal shift of a microwave waveform, the interrogation speed of fiber Bragg grating (FBG) sensors has been increased to MHz range [7,8]. Another application example of PTS is that a high resolution distributed FBG sensor interrogation can be achieved via instantaneous microwave frequency sensing by exploiting the unique wavelength-location mapping in a chirped FBG [9]. However, a special light source such as a mode-locked laser is usually needed in many PTS based interrogation system.

The second type is based on the optoelectronic oscillator (OEO) [10–12], which has drawn lots of attention for its advantages of high speed and high resolution [13,14]. In the OEO-based interrogation scheme, the sensing information can be directly resolved by detecting the frequency of microwave signals generated by the OEO. However, expensive radio frequency devices are needed in the OEO-based interrogation system.

The third type is based on the microwave photonic filter (MPF). The MPF is one of the key elements in microwave photonic systems and normally uses delayed multi-tap optical signals carrying a microwave signal to produce the desired filter response [15,16]. Compared with the interrogation technique based on the PTS and the OEO, the MPF-based interrogation scheme has been adopted widely in the optical sensing field for its simplicity and stable structures. Typically, the use of finite impulse response (FIR) microwave photonic filter on sensing applications has gained ever increasing interest recently [17–20]. Most of the reported interrogation schemes based on FIR-MPF rely on the principle that the measured information is converted to optical delays between different filter taps and the final interrogation results can be obtained from the variation of the microwave photonic filter response. For example, a fiber length sensor [2], a displacement sensor [17], a transverse load sensor [18], and a temperature sensor [19] have been successfully interrogated with high-resolution via the MPF technology. However, the fundamental principle of all these systems is based on uniformly spaced microwave photonic delay line filter, and the target sensing information is mostly demodulated from the change of the free spectral range (FSR) of the filter. Thus only one or two sensors [20] can be interrogated simultaneously in these systems. Although a quasi-distributed hot-spot event sensing system involving multiple optical sensors based on a microwave photonic filter structure has been reported [21], all the sensors are of the same type. More multifunctional interrogation system based on microwave photonic filter structure would be required in order to measure different types of optical sensors. Therefore, a new optical sensor interrogation scheme, which is based on microwave photonic filter, with the capability of measuring different types of sensors in an optical sensor network is highly demanded.

In this work, we report a new design of optical sensor network interrogation platform based on a nonuniformly spaced microwave photonics delay-line filter with nonlinear phase response. The previously reported methods are usually based on uniformly spaced taps technology with linear phase frequency response, thus only the amplitude or the linear phase response is used to demodulate optical sensors. Accordingly, these reported methods can only be utilized to interrogate limited number or types of optical sensors (usually one or two). However, both the amplitude and the phase response of the filter are used to demodulate optical sensors in this proposed method. Therefore, a large sensor network with different types of optical sensors can be interrogated simultaneously. The delay time and the amplitude of each filter tap can be individually modulated by different types of optical sensors embedded in filter taps. Multiple different optical sensors can be interrogated simultaneously from the temporal impulse response of the microwave

Optics EXPRESS

photonic filter. Preliminary results have been presented [22]. More comprehensive analysis and experimental verifications are presented in this paper to further illustrate our proposed method. The experiment results show that there are good linear relationships between the variation of temporal impulse response and the variation of the twist, lateral pressure, transversal loading and temperature, which are consistent with the results of traditional optical spectrum analysis (OSA) measurement. The sensitivity of the sensors in the proposed platform is -2.1301×10^{-5} a.u/degree, 6.1039 ps/kPa, -1.9146×10^{-5} a.u/gram, and 5.1497 ps/°C, respectively.

2. Principle

The operation of the proposed system is based on the generic delay line microwave photonic FIR filter. The FIR filter is built on multiple weighted and delayed optical signals carrying the same microwave signal. In most reported systems [17–20], the interrogation technology is based on uniformly spaced linear-phase MPF. The sensing information is interrogated from the change of the FSR of the MPF. Therefore, only limited number of sensors (no more than two) or multiple sensors of the same type can be measured.

Figure 1 shows the structure of the optical sensor network interrogation system based on the proposed nonuniform microwave photonic filter. There are N arms in the system, and one of the arms works as a reference arm while others work as sensing arms containing optical sensors. Furthermore, an incoherent broadband optical source is adopted in this system in order to make the sensing system resistant to the environmental interference [23]. Meanwhile all the sensors in the network can work simultaneously. The optical filters are employed in the system to obtain the unique wavelength for each arm individually. Multiple optical sensors of different types are utilized in filter taps except the reference one. The electronic transfer function of the filter is given by [16]

$$H(\Omega) = \sum_{k=1}^{N} \alpha_k e^{-j\Omega t_k} \tag{1}$$

where Ω is the angular microwave frequency, N is the number of filter taps, α_k and t_k are the amplitude and time delay of the k^{th} tap, respectively. Combined with the proposed scheme shown in Fig. 1, t_k can be expressed by Eq. (2), in which τ_k is the transmission time of the optical signal along each arm and equals to the length of the optical path divided by the light speed in the fiber and τ_{DIS-k} is the transmission time in the dispersion unit (τ_{DIS-k} equals to the product of the wavelength and the dispersion). The dispersion unit can be used as either a positive dispersion

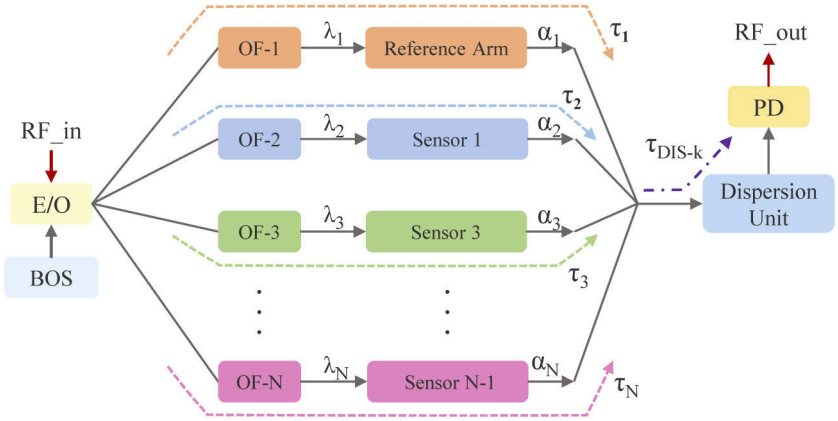


Fig. 1. Schematic of the proposed optical sensor network interrogation system based on nonuniform microwave photonic delay line filter. BOS: broadband optical source. OF: optical filter. E/O: electro-optic conversion unit.

Optics EXPRESS

coefficient device, such as a single-mode fiber [24], or a negative dispersion coefficient device, such as a dispersion compensating fiber (DCF).

$$t_k = \tau_k + \tau_{DIS-k} \tag{2}$$

Optical sensors in sensing arms will modulate the amplitude α_k or the delay time t_k or both of them. Once the difference values between adjacent t_k and t_{k+1} become inconsistent, a nonuniformly spaced microwave photonic delay line filter [25,26] will be formed. As a result, the periodic patterns with fixed FSR of the amplitude response of the filter are destructed and the linearity of the phase response is deteriorated as well. More parameters other than only the FSR can be used to demodulate the sensors embedded in the filter arms. Therefore, more optical sensors can be individually interrogated via inverse Fourier transform of the complete frequency response of the nonuniform microwave photonic filter, and the sensing information can be obtained.

To verify the feasibility of this design, we firstly make a simulation analysis of a four-tap system in which four optical sensors are inserted in the arms (refer to Fig. 4.). It is assumed that the initial state of the system has uniform time delay, and the FSR of the filter is 500 MHz and all the amplitudes of the filter are equal to one. The simulation results of the frequency response of the initial status of system are shown in Fig. 2(a) and Fig. 2(c).

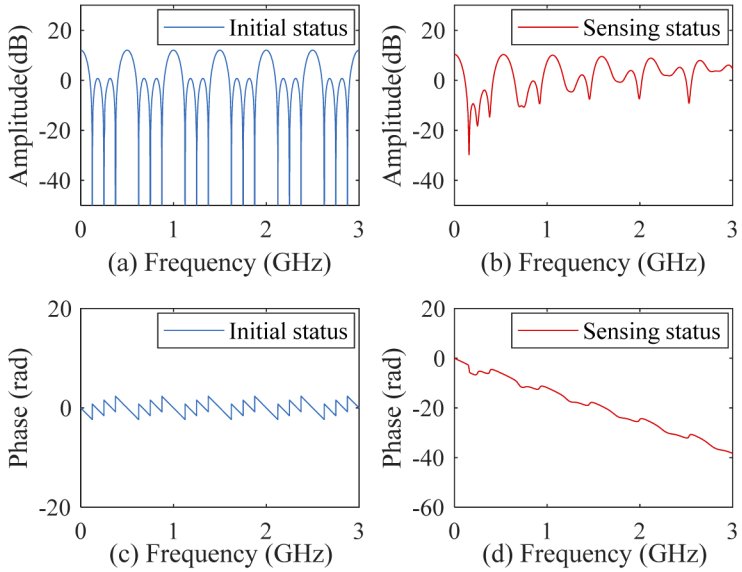


Fig. 2. Simulation results of the frequency response of the designed system. (a) Amplitude frequency response of the initial system. (b)Amplitude frequency response of the sensing system. (c) Phase frequency response of the initial system. (d) Phase frequency response of the sensing system.

In order to obtain a typical analysis of the sensing state of the system, we assume that the second arm works as the reference arm. A twist sensor is assumed to work in the first arm, a lateral pressure sensor is in the third arm, a temperature sensor and a transverse loading sensor are together in the last arm. Based on [27–29], the tilted fiber grating (TFG) can be directly used as an optical sensor and the sensing information can be demodulated from the wavelength shift in its transmission spectrum. The TFG here is used as the twist sensor and it is assumed that the wavelength of the optical signal transmitted into the TFG is fixed, thus only the optical power will change according to the variation of the twist angle. According to [27], when the measuring

Optics EXPRESS

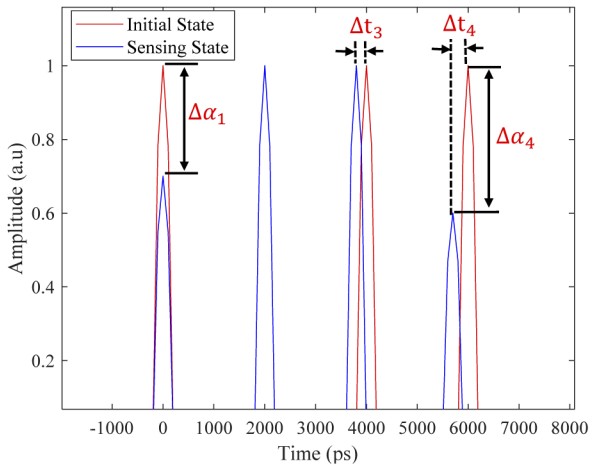


Fig. 3. Simulation result of temporal impulse response of the nonuniformly spaced microwave photonic filter. Red: the initial response after calibration; Blue: updated response representing the optical sensor information.

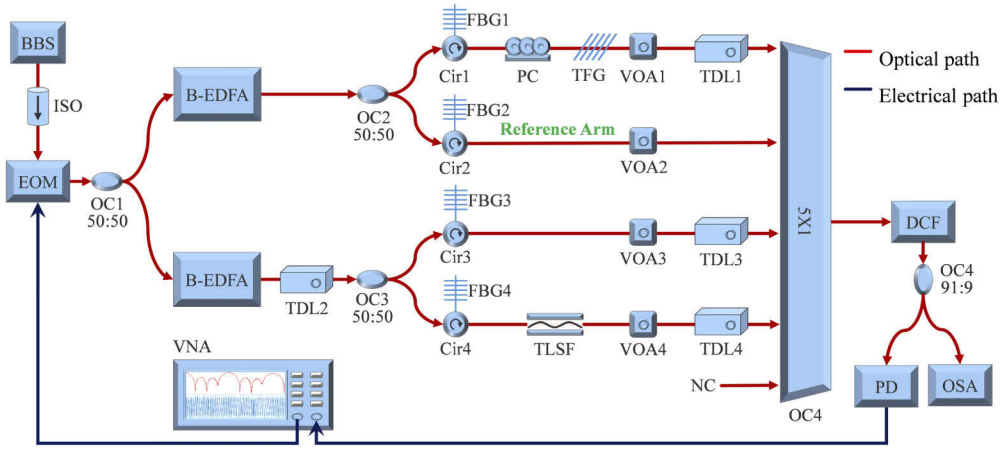


Fig. 4. Experiment setup of the proposed design. BBS: broadband source; ISO: isolator; EOM: electro-optical modulator; OC: optical coupler; B-EDFA: boot-type erbium-doped fiber amplifier; Cir: circulator; TFG: titled fiber grating; VOA: variable optical attenuator; TDL: tunable delay line; TLSF: transverse loading sensing fiber; DCF: dispersion compensating fiber; PD: photo-detector; NC: not connect; OSA: optical spectrum analyzer; VNA: vector network analyzer.

twist angle is between 0° and 180°, there is a linear relationship between the measuring twist angle θ and the amplitude α_k of the tap one, as shown in Eq. (3) and β_1 is a constant decided by TFG. We set the total variation of amplitude α_1 caused by the variation of twist angle equals to 0.3 and the delay time t_1 is set as zero compared to t_2 in the simulation.

$$\theta = \alpha_k/\beta_1 \quad (k = 1) \tag{3}$$

$$P = \beta_2 * \Delta\lambda_k \quad (k = 3) \tag{4}$$

$$\Delta t_k = \Delta\tau_k + D * \Delta\lambda_k \tag{5}$$

Optics EXPRESS

$$P = \frac{\Delta t_k}{D} * \beta_2 \quad (\mathrm{k} = 3) \tag{6}$$

The second arm works as the reference arm, which means that the amplitude α_2 and the delay time t_2 of this arm remain constant. Meanwhile, according to [30], a FBG with a special package can be worked as a lateral pressure sensor, and there is a linear relationship between the lateral pressure P and the wavelength shift $\Delta\lambda_k$, as expressed by Eq. (4), and β_2 is a constant decided by the inherent characteristics of the FBG and the special package. Furthermore, the variation of the delay time Δt_k of k^{th} tap is expressed in Eq. (5), in which D is the dispersion of the dispersion unit. When the length of each arm is fixed, $\Delta\tau_k$ equals to zero, so Eq. (4) can be further expressed as Eq. (6), from which we know that the lateral pressure can be measured by measuring Δt_k. We assume that the total variation of the delay time t_3 equals to 200 ps in the simulation.

$$T = \beta_3 * t_k \quad (\mathrm{k} = 4) \tag{7}$$

$$\varepsilon = \beta_4 * \alpha_k \quad (\mathrm{k} = 4) \tag{8}$$

The last arm is supposed to contain two types of optical sensors: a FBG sensor to measure the temperature change and a sensor based on a single mode fiber (SMF) to measure the transverse loading. According to [31], there is a linear relationship between the temperature T and the delay time t_k, as shown in Eq. (7). The transverse loading ε and the amplitude α_k also have a linear relationship, as shown in Eq. (8). In the simulation, we assume that the variation of t_4 equals to 300 ps and the variation of α_4 equals to 0.4, respectively.

The simulation parameters are summarized and shown in Table 1. The simulation results of the frequency response of the sensing status of the system are shown in Fig. 2(b-d). From Fig. 2(a) we can see that four uniformly spaced taps with a FSR of 500 MHz is realized in the initial state. Figure 2(c) shows a linear relationship for the phase-frequency response of the initial state. However, the periodic patterns with fixed FSR of the amplitude response of the filter are destructed and the linearity of the phase response is deteriorated in sensing state, as shown in Fig. 2(b) and Fig. 2(d) respectively.

Table 1. Simulation parameters setting

Sensor	TFG (arm1)	Reference (arm2)	FBG3 (arm3)	FBG4 (arm4)	SMF (arm4)
Initial status	$\alpha_1 = 1$	$\alpha_2 = 1$	$\alpha_3 = 1$	$t_4 = 6000ps$	$\alpha_4 = 1$
	$t_1 = 0ps$	$t_2 = 2000ps$	$t_3 = 4000ps$		
Sensing status	$\alpha_1 = 0.7$	$\alpha_2 = 1$	$\alpha_3 = 1$	$t_4 = 5700ps$	$\alpha_4 = 0.6$
	$t_1 = 0ps$	$t_2 = 2000ps$	$t_3 = 3800ps$		
Variations	$\Delta\alpha_1 = 0.3$	Constant	$\Delta t_3 = 200ps$	$\Delta t_4 = 300ps$	$\Delta\alpha_4 = 0.4$

After the inverse Fourier transform of the frequency response of the filter, the simulation results of sensing information was obtained, as shown in Fig. 3. The initial response of the system is shown in red while the sensing response is shown in blue. By comparing the change of the amplitude α_k and the delay time t_k respectively, all the measuring information (θ, P, T, ε) can be interrogated simultaneously. The simulation results are consistent with the theoretical analysis. It should be noted that the influence of optical filters' bandwidths on the pulse signals in time domain should be considered in simulation.

3. Experimental results and discussions

To further verify the feasibility of the proposed design, experiments is carried out based on the setup shown in Fig. 4. Light emitted from the broadband light source (Hoyatek ASE-C-N) is

Optics EXPRESS

modulated by a microwave signal from the vector network analyzer (VNA, Keysight E5071C, frequency sweep range: 100 KHz ~ 8.5 GHz) at the Mache-Zehnder modulator (MZM, Conquer KG-AM-15). Then the modulated optical signal is firstly divided into two paths by the first optical coupler (OC1), and the signals in the upper path and the lower path are amplified by two boost-type erbium-doped fiber amplifiers (B-EDFA, MAX-RAY Photonic EDFA-BA-26), respectively. Filter taps are formed based on the spectrum slicing by using narrow-band uniform fiber Bragg gratings (FBGs) in each filter arms. In our design, FBG1 and FBG2 are only working as the spectral filtering device, while FBG3 and FBG4 not only serve as the filtering devices but also work as optical sensors. Therefore, four taps are formed and then optical signals in four paths are combined at OC4. Here variable optical attenuators (VOAs) and tunable delay lines (TDLs, Conquer ODL-300) are contained for the initial calibration purpose. The dispersion of the combined signals is compensated by the DCF (Yangtze Inc. −497 ps/nm@1545nm). Finally, optical signals are divided into two parts by OC5 (91:9), and 91% of the optical signals power are converted into the electrical signals by the photo-detector (PD, Conquer KG-PT-40G), then sent to the VNA. The rest 9% are observed by OSA (YOKOGAWA AQ 6370D).

The designed system is configured to have uniformly spaced filter taps at the beginning and all the sensors in the arms play the same role as described in section 2. As mentioned above, the TFG in the first arm works as a twist senor, the second arm works as the reference arm, the FBG3 in the third arm works as a lateral pressure sensor, the FBG4 and a common single mode fiber in the last arm work as the temperature sensor and the transverse loading sensor, respectively. In Fig. 5(a), the TFG is twisted by rotating one of the two three-axis stages (Thorlabs Inc.). The FBG3 is wrapped with Polydimethylsiloxane (PDMS) and then packaged with a 3D printed special clamp to achieve the lateral pressure sensing as shown in Fig. 5(b). In Fig. 5(c), the FBG4 is fixed into the dry bath (Allsheng MK-20) to measure the temperature variations. A section of single mode fiber is put into a 3D printed clamp with two occlusal layers to measure the transverse loading, as shown in Fig. 5(d).

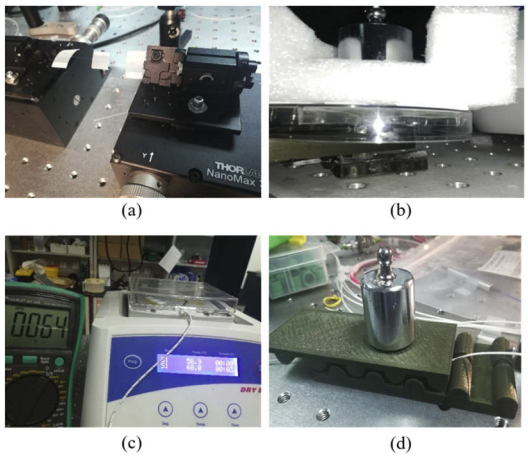


Fig. 5. (a) TFG work as a twist sensor on the three-axis stages. (b) FBG3 is wrapped with PDMS and packaged with a special clamp. (c) FBG4 is fixed into the dry bath to measure the temperatures. (d) A section of single mode fiber into a special clamp with two occlusal layers is used to measure the transverse loading.

In order to demonstrate the performance of this proposed design, as shown in Fig. 4, the sensing information is interrogated by the traditional OSA method and this proposed method simultaneously. Single-measurement and multiple-measurement experiments are described in section 3.1 and 3.2 respectively.

Optics EXPRESS

3.1. Single-measurement results

Firstly, the single measurement of the corresponding measurand for each sensor is performed simultaneously, in order to explain the operation principle of the proposed system in detail. The applied measurand to each sensor is described as follows: 60 degrees of twist are applied to the TFG, the second arm remain constant, 30.8kPa pressure is pressed on PDMS that packages the FBG3, 50-gram weight is pressed on the clamp that contains the transverse loading sensor and the temperature applied to the temperature sensor is 60°C. Figure 6 shows the measured optical spectrum of the preliminary validation. It can be seen that there are four red waveforms in the initial status, and the wavelength of the waveforms from left to right is 1550.07nm (−44.58dBm), 1553.01nm (−44.39dBm), 1555.65nm (−44.52dBm) and 1559.07nm (−44.61dBm). The applied signals can be demodulated by comparing the waveform changes between the initial and the sensing status: the amplitude of the first waveform falls down (1550.07nm@−46.88dBm), which is resulted from the decrease of the transmitted optical power when the TFG in the first arm is twisted. The second waveform remains consistent with the reference role of the second arm. There exists a red shift of the third waveform (1556.13nm@−44.16dBm), in response to a lateral pressure measured by FBG3 in the third arm. There are also a red shift and an amplitude decline of the fourth waveform (1559.54nm@−44.97dBm), which are caused by the temperature sensor FBG4 and the transverse loading sensor in the final arm respectively. The change of the optical spectrum is consistent with the previous analysis in section 2.

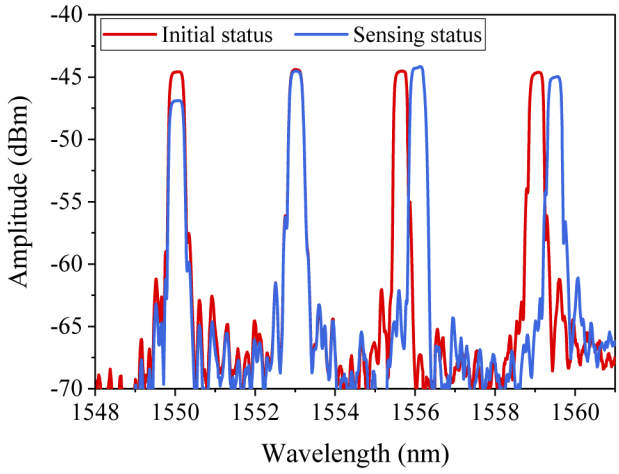


Fig. 6. The measured optical spectrum of the preliminary validation.

The radio frequency (RF) scan range adopted in the experiment is from 100 KHz to 5 GHz. We selected a section length of one FSR to analyze the response of the system, as shown in Fig. 7(a) and (b). Figure 7(a) shows four uniformly spaced taps with a FSR of 465 MHz are realized in the initial state. Meanwhile the nonuniform taps are formed when the sensing information is applied to this sensing network, as shown in Fig. 7(b). In order to analyze the frequency response more clearly, one pass-band of the amplitude-frequency response is selected, as shown in Fig. 7(c)-(f), and the corresponding phase-frequency responses are shown in Fig. 7(e) and Fig. 7(f), respectively. Then the linear fitting is performed for these two phase frequency responses respectively, and the results show that the norm of residuals for fitting the phase-frequency response in the initial state is 0.23669, while 0.83052 for the sensing state. Therefore, the linearity of the phase-frequency response of the system in the sensing state is worse than that in the initial state. This is consistent with the prediction of the previous simulation.

Optics EXPRESS

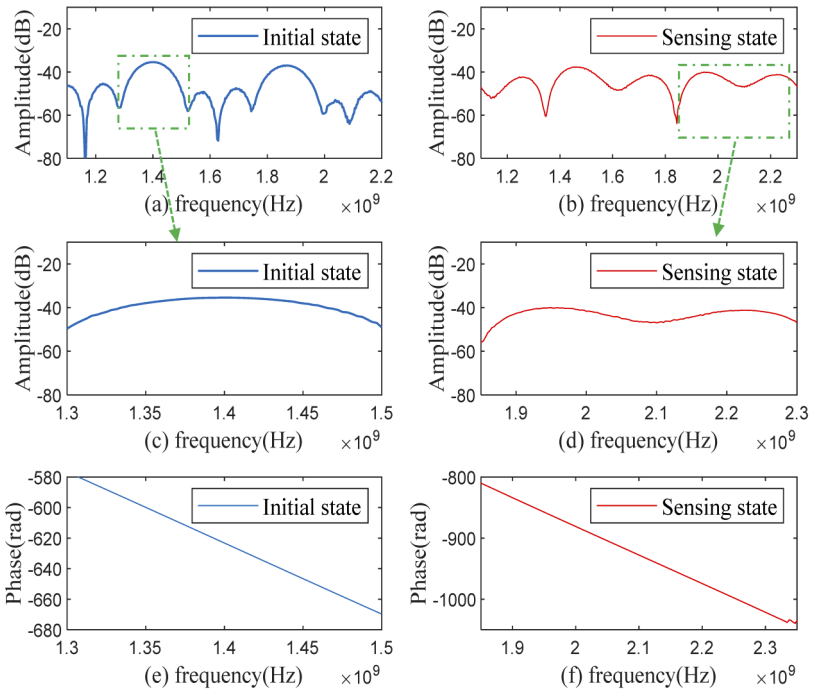


Fig. 7. Experiment results of the frequency response of the system. (a) amplitude-frequency response of the system in initial state in one FSR range. (b) amplitude-frequency response of the system in sensing state in corresponding range. (c) amplitude-frequency response of the system in initial state in one pass-band. (d) amplitude-frequency response of the system in sensing state in one pass-band. (e) phase-frequency response of the system corresponding to (c). (d) phase-frequency response of the system corresponding to (d).

The temporal impulse response of the proposed filter is obtained via inverse Fourier transform of the frequency response with the results shown in Fig. 8. Comparing Fig. 3 with Fig. 8, we can see that the variation trend of the experiment results is consistent with the variation trend of the simulation results. In Fig. 8, the variations of the four blue waveforms from left to right relative to the red waveforms are as follows: the peak value of the first waveform is reduced by 1.402e–03au, the second waveform remains the same, the third peak has a blue shift of ~200ps, and the last waveform also has a blue shift of ~200ps and its peak value is reduced by 3.32e–04au. Note that the third peak in blue on the left is higher than the corresponding red peak, and this may be due to a slight lateral distortion of FBG under the pressure, resulting in a higher reflected optical power than in the initial state. However, this does not affect the measurement results, as we focus on the shift of this peak rather than its amplitude variation.

3.2. *Multiple-measurement results*

In order to further verify the performance of the system, multiple variations of the four measurands corresponding to four sensors are measured. The applied variations of the measurands to each sensor are described as follows: the twist from 20 degrees to 100degrees with a step of 20 degrees is applied for the twist measurement; the weight from 200 gram to 800 gram with a step of 200 gram is placed on a fixed circular contact surface with the diameter of 9mm, respectively, so the corresponding pressures of 30.8 kPa, 61.6 kPa, 92.4 kPa and 123.2 kPa are obtained for the lateral pressure measurement; the weight from 50 gram to 130 gram with a step of 20 gram is

Optics EXPRESS

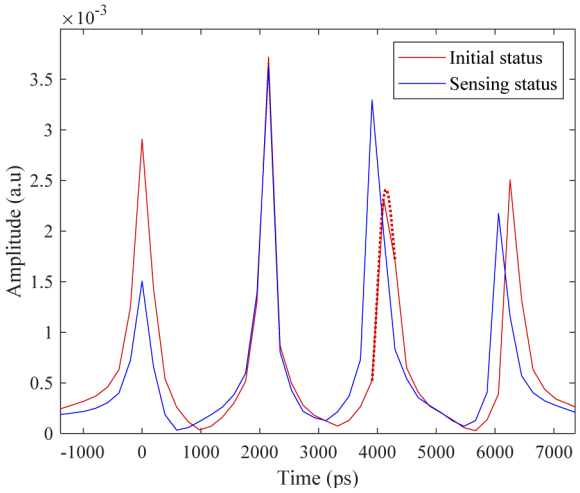


Fig. 8. Temporal impulse response of the nonuniformly spaced microwave photonic filter based on measured value. Red: the initial response after calibration; Blue: updated response representing the optical sensor information. The dotted line of the third peak indicates the processing of interp.

applied for the transversal loading measurement; the temperature of 20°C, 40°C, 60°C, 80°C and 97°C is applied to the temperature sensor.

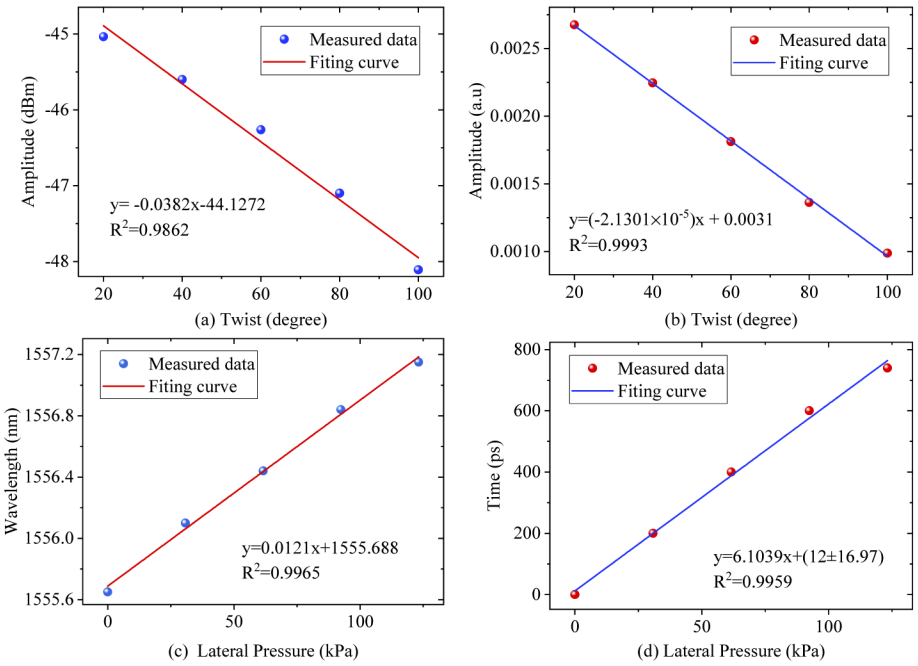


Fig. 9. The comparison of the experimental results of the two methods used to measure twist and lateral pressure, including the twist measured by OSA (a), the twist measured by this proposed MPF method (b), the lateral pressure measured by OSA (c), and the lateral pressure measured by this proposed MPF method (d).

Optics EXPRESS

The measured results are shown in Fig. 9(a)-(d) and Fig. 10(a)-(d). The original data measured by the MPF method and its data processing codes are shown in Dataset 1 (Ref. [32]) and Code 1 (Ref. [33]), respectively. The experiment results obtained by the proposed MPF methods is consistent with those obtained by OSA, showing good linearity between the measurands and the sensing parameters. These prove the feasibility of this proposed method and the performance of the system. Moreover, once the system is calibrated, the measured changes can be derived from the temporal signal changes.

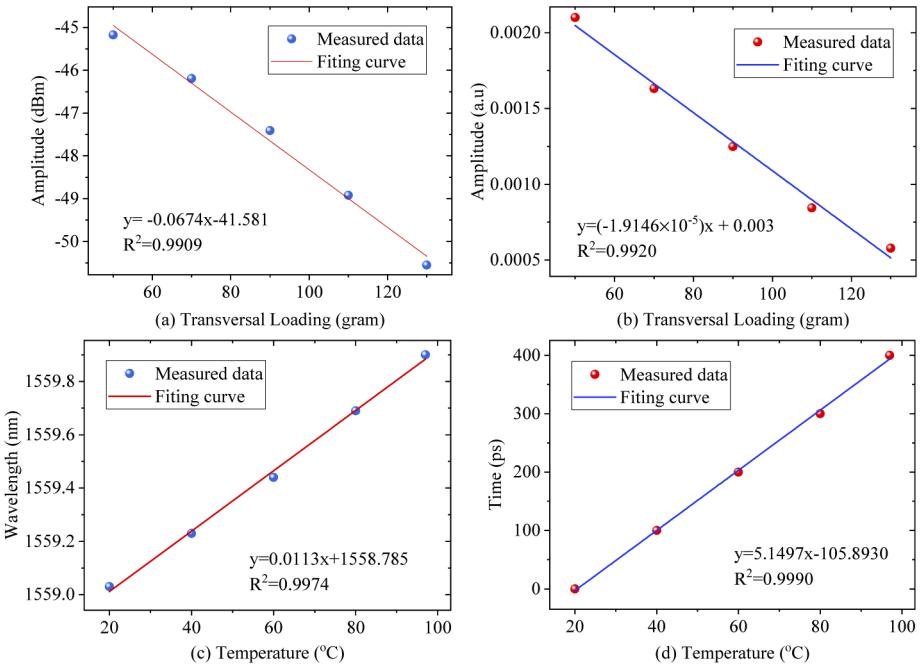


Fig. 10. The comparison of the experimental results of the two methods used to measure transversal loading and temperature, including the transversal loading measured by OSA (a), the transversal loading measured by this proposed MPF method (b), the temperature measured by OSA (c), and the temperature measured by this proposed MPF method (d).

3.3. Discussions

Although the experimental comparisons show that the measured results of the proposed method has the same linearity like the results of the other one, there are some differences between the two methods. Firstly, the OSA can only support the measurement of the amplitude and the wavelength. While in addition to the ability of measuring the variations of the amplitude and the wavelength, our proposed method is also capable of measuring the absolute delay time, such as the absolute delay generated by the micro-displacement optical fiber sensors, where the wavelength is constant, but there is indeed a delay (optical path difference). This can be explained by Eq. (5): When the parameter $\Delta\lambda_k$ equals to zero, the parameter $\Delta\tau_k$ caused by the optical path difference only equals to Δt_k which can be expressed by the variation of the temporal impulse. Secondly, for the wavelength measurement, the OSA method can only get an "unprocessed value" or "intrinsic value". For example, the variation of 0.01nm of the wavelength can only be "seen" as 0.01nm by the OSA, but the proposed method is able to "amplify the variation of the wavelength", which can be more useful to measure the small variation in wavelength. This can also be explained by Eq. (5), in which the variations of the wavelength is amplified by the dispersion value D (its

Optics EXPRESS

absolute value is much greater than one). Therefore, our approach can achieve the functions that OSA does not have.

More importantly, this proposed method provides a potential centralized demodulation platform, with the ability of interrogating lots of optical sensors of different types simultaneously.

In addition, the scan time range is determined by the frequency step, and the time scan accuracy is determined by the maximum frequency sweep range. The higher the frequency sweep range, the higher the accuracy. In the experiment, the frequency sweep range is set as 5 GHz. Then, the equivalent frequency sweep range after the IFFT operation is 10 GHz (because ±5 GHz is concluded in the complex domain), and the corresponding time resolution is 100 ps, which is sufficient for our system. The accuracy can be further improved by increasing the dispersion of the system or using a VNA with a larger frequency sweep range. In addition, the whole system has a relatively high tolerance of signal to noise ratio (SNR), because what we focus on is the change of the entire envelope shape of the filter response.

4. Conclusion

In summary, a new optical sensor network interrogation platform based on nonuniformly spaced microwave photonic delay-line filter is proposed and experimentally demonstrated. Four optical sensors of different types are contained in the system to simultaneously measure the variation of the twist, the lateral pressure, the transversal loading and the temperature. The sensing information is obtained from the complex temporal impulse response of the sensor-embedded microwave photonic filter. The measurement sensitivity of the sensors in the proposed platform is -2.130×10^{-5} a.u/degree, 6.1039 ps/kPa, -1.9146×10^{-5} a.u/gram, and 5.1497 ps/°C, respectively. The sensitivity can be further improved by optimizing the packaging of the sensors, or setting the initial FSR of the system at a lower value. Proper packages for fiber sensors can increase the sensitivities of the sensors to the variation of measurands, but in the experiment, the sensors used to measure the twist and temperature are not packaged at all, and the sensors used to measure the lateral pressure and transversal loading are only with very rough and very simple packages, so perceptions of these sensors to the measurands are actually not very good. On the other hand, the lower FSR value is corresponding to a larger variation in the time domain, therefore, for the wavelength-measurement optical fiber sensors, the lower FSR value corresponds to the larger time variation in time domain. Hence, the sensitivity can be further improved. In a more practical situation, the interrogation system can be much smaller using the compact modules. More importantly, this centralized interrogation platform can be remotely connected to and shared by all optical sensors in the whole sensor network. Therefore, large-scale optical sensor network interrogation can be supported by the same compact interrogation system.

Funding. Southern University of Science and Technology (Y01236128); Engineering and Physical Sciences Research Council (EP/S005625/1); The Verification Platform of Multi-tier Coverage Communication Network for Oceans (LZC0020); PCL Future Greater-Bay Area Network Facilities for Large-scale Experiments and Applications (LZC0019).

Disclosures. The authors declare no conflicts of interest.

References

1. B. Culshaw, "Optical fiber sensor technologies: Opportunities and-perhaps-pitfalls," J. Lightwave Technol. **22**(1), 39–50 (2004).
2. J. Hervas, A. L. Ricchiuti, W. Li, N. H. Zhu, C. R. Fernandez-Pousa, S. Sales, M. Li, and J. Capmany, "Microwave Photonics for Optical Sensors," IEEE J. Sel. Top. Quantum Electron. **23**(2), 327–329 (2017).
3. J. P. Yao, "Microwave Photonics for High-Resolution and High-Speed Interrogation of Fiber Bragg Grating Sensors," Fiber Integr. Opt. **34**(4), 204–216 (2015).
4. S. X. Chew, X. K. Yi, W. J. Yang, C. J. Wu, L. W. Li, L. Nguyen, and R. Minasian, "Optoelectronic Oscillator Based Sensor Using an On-Chip Sensing Probe," IEEE Photonics J. **9**(2), 1–9 (2017).
5. M. G. Wang, N. H. Zhang, X. D. Huang, B. Yin, H. Q. Mu, M. Y. Han, and D. S. Chen, "High sensitivity demodulation of a reflective interferometer-based optical current sensor using an optoelectronic oscillator," Opt. Lett. **45**(16), 4519–4522 (2020).

Optics EXPRESS

6. D. W. Zhou, Y. K. Dong, and J. P. Yao, "Truly Distributed and Ultra-Fast Microwave Photonic Fiber-Optic Sensor," J. Lightwave Technol. **38**(15), 1 (2020).
7. W. L. Liu, M. Li, C. Wang, and J. P. Yao, "Real-Time Interrogation of a Linearly Chirped Fiber Bragg Grating Sensor Based on Chirped Pulse Compression With Improved Resolution and Signal-to-Noise Ratio," J. Lightwave Technol. **29**(9), 1239–1247 (2011).
8. M. Lei, W. W. Zou, X. Li, and J. P. Chen, "Ultrafast FBG Interrogator Based on Time-Stretch Method," IEEE Photonics Technol. Lett. **28**(7), 778–781 (2016).
9. E. J. Ahmad, C. Wang, D. J. Feng, Z. J. Yan, and L. Zhang, "High Temporal and Spatial Resolution Distributed Fiber Bragg Grating Sensors Using Time-Stretch Frequency-Domain Reflectometry," J. Lightwave Technol. **35**(16), 3289–3295 (2017).
10. X. H. Zou, X. K. Liu, W. Z. Li, P. X. Li, W. Pan, L. S. Yan, and L. Y. Shao, "Optoelectronic Oscillators (OEOs) to Sensing, Measurement, and Detection," IEEE J. Quantum Electron. **52**(1), 1–16 (2016).
11. F. Z. Zhang, P. Zhou, B. D. Gao, and S. L. Pan, "Multi-frequency Optoelectronic Oscillators: Realization and Applications," *2016 Progress in Electromagnetics Research Symposium* (Piers), 1634 (2016).
12. D. Q. Feng, L. Kai, T. Zhu, Y. Gao, L. Gao, and J. D. Zhang, "High-precision strain-insensitive temperature sensor based on an optoelectronic oscillator," Opt. Express **27**(26), 37532–37540 (2019).
13. J. P. Yao, "Optoelectronic Oscillators for High Speed and High Resolution Optical Sensing," J. Lightwave Technol. **35**(16), 3489–3497 (2017).
14. Z. W. Xu, X. W. Shu, and H. Y. Fu, "Fiber Bragg grating sensor interrogation system based on an optoelectronic oscillator loop," Opt. Express **27**(16), 23274–23281 (2019).
15. R. A. Minasian, "Photonic signal processing of microwave signals," IEEE Trans. Microwave Theory Tech. **54**(2), 832–846 (2006).
16. J. Capmany, B. Ortega, and D. Pastor, "A tutorial on microwave photonic filters," J. Lightwave Technol. **24**(1), 201–229 (2006).
17. L. W. Li, X. K. Yi, S. X. Chew, S. J. Song, L. Nguyen, and R. A. Minasian, "Double-pass microwave photonic sensing system based on low-coherence interferometry," Opt. Lett. **44**(7), 1662–1665 (2019).
18. Y. P. Wang, M. Wang, W. Xia, and X. Q. Ni, "High-resolution fiber Bragg grating based transverse load sensor using microwave photonics filtering technique," Opt. Express **24**(16), 17960–17967 (2016).
19. Z. W. Xu, X. W. Shu, and H. Y. Fu, "Sensitivity enhanced fiber sensor based on a fiber ring microwave photonic filter with the Vernier effect," Opt. Express **25**(18), 21559–21566 (2017).
20. S. Y. Li, R. Wu, H. Wang, X. Y. Chen, P. P. Fu, H. Y. Fu, Y. F. Wang, H. Y. Xu, and Z. P. Cai, "Fiber-Ring-Based RF Filtering for Temperature and Transversal Loading Measurement and Interrogation," IEEE Sens. J. **18**(14), 5794–5798 (2018).
21. A. L. Ricchiuti, D. Barrera, S. Sales, L. Thevenaz, and J. Capmany, "Long fiber Bragg grating sensor interrogation using discrete-time microwave photonic filtering techniques," Opt. Express **21**(23), 28175–28181 (2013).
22. D. Xiao, T. Han, L. Shao, and C. Wang, "Nonuniform Microwave Photonic Delay-Line Filter For Optical Sensor Network Interrogation," International Topical Meeting on Microwave Photonics (MWP) (2019).
23. J. Capmany, J. Mora, I. Gasulla, J. Sancho, J. Lloret, and S. Sales, "Microwave Photonic Signal Processing," J. Lightwave Technol. **31**(4), 571–586 (2013).
24. X. Y. Dong, L. Y. Shao, H. Y. Fu, H. Y. Tam, and C. Lu, "Intensity-modulated fiber Bragg grating sensor system based on radio-frequency signal measurement," Opt. Lett. **33**(5), 482–484 (2008).
25. Y. T. Dai and J. P. Yao, "Nonuniformly Spaced Photonic Microwave Delay-Line Filters and Applications," IEEE Trans. Microwave Theory Tech. **58**(11), 3279–3289 (2010).
26. C. Wang and J. P. Yao, "A Nonuniformly Spaced Microwave Photonic Filter Using a Spatially Discrete Chirped FBG," IEEE Photonics Technol. Lett. **25**(19), 1889–1892 (2013).
27. X. Chen, K. Zhou, L. Zhang, and I. Bennion, "In-fiber twist sensor based on a fiber Bragg grating with 81 degrees tilted structure," IEEE Photonics Technol. Lett. **18**(24), 2596–2598 (2006).
28. L. Y. Shao and J. Albert, "Lateral force sensor based on a core-offset tilted fiber Bragg grating," Opt. Commun. **284**(7), 1855–1858 (2011).
29. J. Albert, L. Y. Shao, and C. Caucheteur, "Tilted fiber Bragg grating sensors," Laser Photonics Rev. **7**(1), 83–108 (2013).
30. H. J. Sheng, M. Y. Fu, T. C. Chen, W. F. Liu, and S. S. Bor, "A lateral pressure sensor using a fiber Bragg grating," IEEE Photonics Technol. Lett. **16**(4), 1146–1148 (2004).
31. S. W. Zhang, R. Wu, H. Chen, H. Y. Fu, J. Li, L. Zhang, M. Zhao, and D. Zhang, "Fiber-Optic Sensing Interrogation System for Simultaneous Measurement of Temperature and Transversal Loading Based on a Single-Passband RF Filter," IEEE Sens. J. **17**(7), 2036–2041 (2017).
32. D. R. Xiao, L. Y. Shao, C. Wang, H. Lin, F. H. Yu, G. Q. Wang, T. Ye, W. Z. Wang, and M. I. Vai, "Data of Multiple-measurement-MPF," figshare (2020), https://doi.org/10.6084/m9.figshare.13200482
33. D. R. Xiao, L. Y. Shao, C. Wang, H. Lin, F. H. Yu, G. Q. Wang, T. Ye, W. Z. Wang, and M. I. Vai, "Codes of Multiple-measurement-MPF, " figshare (2020), https://doi.org/10.6084/m9.figshare.13200503